Cross-Linking of *trans* Reentrant Loops in the Na$^+$-Citrate Transporter CitS of *Klebsiella pneumoniae*[†]

Adam Dobrowolski and Juke S. Lolkema*

Molecular Microbiology, Groningen Biomolecular Sciences and Biotechnology Institute, University of Groningen, Groningen, The Netherlands

ABSTRACT: The membrane topology model of the Na$^+$-citrate transporter CitS of *Klebsiella pneumoniae* shows a core of two homologous domains with opposite orientation in the membrane and each containing a so-called reentrant loop. A split version of CitS was constructed to study domain interactions and proximity relationships of the putative reentrant loops. Split CitS retained 50% transport activity of the wild-type version in membrane vesicles. Unspecific cross-linking of the purified complex with glutaraldehyde revealed a tetrameric complex with two N and two C domains corresponding to dimeric CitS. The separately expressed domains were not detected in the membrane. Strong interaction between the two domains followed from successful purification of the whole complex by Ni^{2+}-NTA chromatography when only one domain was His-tagged. The presence of citrate and/or the co-ion Na$^+$ during purification did not seem to affect the interaction significantly. Successful disulfide cross-linking was obtained between single cysteine residues introduced in the highly conserved GGNG sequence motif at the vertex of the reentrant loop in the N domain and either of two endogenous cysteine residues at the base of the reentrant loop in the C domain. The disulfide bond was formed within one subunit in the dimer. A model is proposed in which the reentrant loops in the N and C domains are overlapping at the domain interface in the 3D structure where they form (part of) the translocation pathway for substrate and co-ions.

The 2-hydroxycarboxylate transporter family (2HCT[1] TC 2. A.24 (*1*)) is a family of secondary transporters found exclusively in bacteria. Members of the family transport substrates that contain the 2-hydroxycarboxylate motif, as in citrate, lactate, and malate (*2*). As in other families of secondary transporters, the members of the 2HCT family represent different modes of energy coupling. The transporters are either H$^+$ or Na$^+$ symporters or they catalyze exchange between two substrates. More or less characterized members of the family include the Na$^+$ symporters CitS of *Klebsiella pneumoniae* and MaeN of *Bacillus subtilis*, the H$^+$ symporters CimH of *B. subtilis* and MalP of *Streptococcus bovis*, the citrate/acetate exchanger CitW of *K. pneumoniae*, and the malate/lactate exchanger MleP and citrate/lactate exchanger CitP both found in lactic acid bacteria.

The 2HCT family is found in class ST[3] in the MemGen system that classifies membrane proteins in structural classes based on hydropathy profile analysis (*3−6*). Proteins in the different families in a structural class in the MemGen system are not related in sequence but are believed to share the same global folding and, most likely, the same mechanism. Support for the approach was recently obtained for different families in classes ST[2] (*7, 8*) and ST[3] (*9, 10*). Class ST[3] contains 32 families of secondary transporters including the ion transporter (IT) superfamily (*11*). No high-resolution 3D structure is available for any of the >10000 transporters found in the public databases that belong to structural class ST[3]. Therefore, information on the structure and mechanism of 2HCT transporters bears upon an important group of transporter families for which an X-ray structure is still elusive.

By far the best studied transporter in the 2HCT family is the Na$^+$-citrate symporter CitS of *K. pneumoniae*. Studies on mostly CitS have resulted in a detailed structural model for the transporters in the family (*2, 12, 13*). The proteins exist as dimers in the membrane (*14*). The monomeric subunit consists of 11 transmembrane segments (TMSs) with the N- and C-termini at the cytoplasmic and periplasmic side of the membrane, respectively (see Figure 1A). The N-terminal TMS is not part of the core structure and is absent in most other families of structural class ST[3]. The core structure is formed by two homologous domains of five TMSs that each share a similar fold but have opposite orientation in the membrane (*15, 16*). Inverted topology of homologous domains is a structural motif observed in transporters of several other nonrelated families, i.e., aquaporin (*17*), the Na$^+$/H$^+$ antiporter NhaA (*18*), the ammonium transporter AmtB (*19*), and the Na$^+$-leucine transporter LeuT (*20*). The two domains are believed to originate from an ancient duplication of a gene encoding an odd number of TMSs (*21*). The loops between the fourth and fifth transmembrane segment in each domain in the 2HCT family model form so-called pore loops or reentrant loops, which fold back in between the transmembrane segments from opposite sides of the membrane (*trans* reentrant loops). Embedded in a different structural context, a similar pair of reentrant loops is observed in the structures of aquaporins (*17*)

*Corresponding author. Tel: +31 50 363 2155. Fax: +31 50 363 2154. E-mail: j.s.lolkema@rug.nl.
[1]Abbreviations: 2HCT, 2-hydroxycarboxylate; TMS, transmembrane segment; RSO, right side out; FM, fluorescein-5-maleimide; GA, glutaraldehyde; NaTT, sodium tetrathionate; TFA, trifluoroacetic acid.
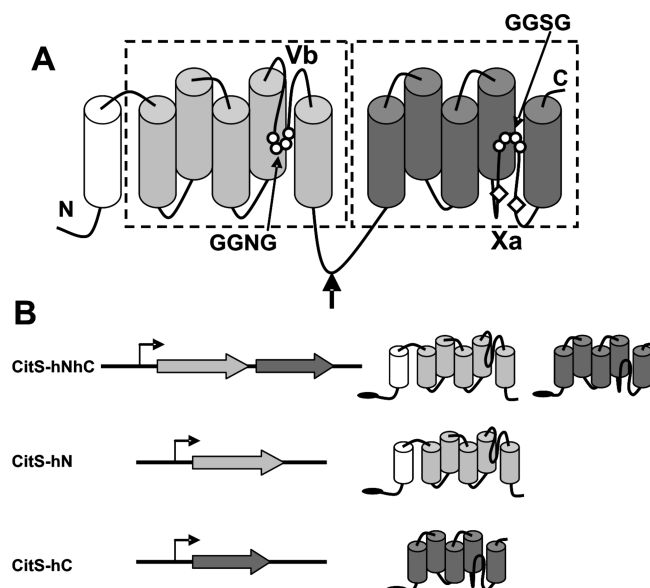
FIGURE 1: Schematic representation of (A) the structural model of CitS of *Klebsiella pneumoniae* and (B) the genetic constructs used to express split CitS and the separate domains. (A) Dashed boxes represent the N and C domains containing five TMSs (cylinders) that together form the core structure of CitS. Two reentrant loops termed Vb and Xa enter the membrane-embedded part of the protein from the periplasmic and cytoplasmic side of the membrane, respectively. Sequence motifs GGNG and GGSG at the vertex of the reentrant loops were indicated by open dots. Two endogenous cysteine residues in reentrant loop Xa were indicated by open diamonds. The two homologous domains are connected by a long cytoplasmic loop. The arrow indicates the site where CitS was split yielding split CitS. (B) Operon structures are shown at the left and the encoded proteins at the right. Closed ovals at the N-termini of the proteins represent His tags.

and the glutamate transporter homologue of the archaeon *Pyrococcus horikoshi* (*22*). The vertexes of the reentrant loops of the 2HCT transporters are formed by GGXG sequence motifs that were shown to be crucial for transport activity (*8*). Aspects of the model are supported by membrane topology studies, cysteine accessibility studies, mutagenesis studies, and kinetic analyses that were recently reviewed in (*2*) or presented in subsequent papers (*8, 9, 14*).

An appealing hypothesis (*2*) positions the reentrant loops in the N and C domains in the structural model of the 2HCT transporters at the interface of the two domains where they would constitute the translocation pathway for substrate and co-ions. In this paper this possibility is addressed by cross-linking studies using a split permease approach (*23*). It is shown that a CitS variant genetically split in between the two domains forms a stable complex in the membrane that is active in Na^+-coupled citrate transport and that retains its quaternary structure after purification from the membrane. In the purified complex, the two domains could be chemically cross-linked by disulfide bond formation between cysteine residues positioned in the two reentrant loops.

EXPERIMENTAL PROCEDURES

Bacterial Strains, Growth Conditions, and Expression of CitS Derivatives. *Escherichia coli* strain DH5α was routinely grown in Luria−Bertani broth (LB) medium at 37 °C under continuous shaking at 150 rpm. Ampicillin was used at a final concentration of 50 μg/mL. CitS and split CitS versions were expressed in *E. coli* DH5α cells harboring plasmid pBAD24

(Invitrogen) derivatives (*24*). The proteins were extended with six additional histidine residues at the N-terminus (His tag) and enterokinase cleavage site unless otherwise stated. Expression of genes cloned in pBAD24 is under control of the arabinose promoter. Production of the proteins was induced by addition 0.01% arabinose when the optical density of the culture measured at 660 nm (OD_{660}) reached a value of 0.6.

Construction of Split citS Genes. All genetic manipulations were done in *E. coli* DH5α cells. Plasmid pCitS-hNC was constructed by PCR insertion mutagenesis. Synthetic primer 5′-GGGGAACTGGTGCGTAAA**TAA**GCTAGCA**GGAGG**-AATTCACC**ATG**GCCTCGTTCAAAGTGG-3′ was designed to insert a sequence containing a termination codon, a ribosomal binding site (RBS), and a start codon (marked in bold) into the *citS* gene in plasmid pBAD-CitS (*24*) between the codons encoding K249 and A250 in the CitS protein (underlined bases correspond to sequences in the *citS* gene). Plasmid pCitS-hNC encodes a protein containing the N-terminal 249 amino acid residues of the CitS protein (N domain plus TMSI) extended with a N-terminal His tag and enterokinase cleavage site and a protein consisting of the C-terminal 198 amino acid residues of CitS (C domain; see also Figure 1B). Plasmid pCitS-hC was constructed by deleting a *NcoI−NcoI* fragment from pCitShNC which results in a single gene encoding the C domain extended with the His tag and enterokinase cleavage site at the N-terminus. The pCitS-hN vector was constructed by first inserting by PCR a sequence containing a *SmaI* restriction site between the stop codon of the N domain and the RBS upfront the C domain in the pCitS-hNC vector. Subsequent deletion of a *SmaI/MscI* fragment yields pCitS-hN. Plasmid pCitS-hNhC was constructed by ligating a *NheI* fragment excised from pCitS-hNC into pCitS-hC digested with the same restriction enzyme. Plasmid pCitS-NhC was constructed by ligating a *Bpu*1102I/*SalI* fragment from pCitS-hNhC into a pBAD24 vector containing the *citS* gene without the His tag and enterokinase site (unpublished). Plasmid pSSSCC-hNhC was constructed by ligating the *Bpu*1102I/*StuI* fragment from pCitSCysless-hNhC, made in similar steps as pCitS-hNhC but with the Cys-less version of the *citS* gene, vector into similarly digested pCitS-hNhC. Plasmid pSSSCC-183-hNhC and the other mutants with Cys inserted in the GGGNG motif of the Vb region and two native cysteines in the Xa region were constructed by cloning *Bpu*1102I/*SpeI* fragments from pSSSCC-hChN construct into similarly digested pCitS-G183C (*8*). All plasmids were sequenced and shown to contain the desired constructs (ServiceXS, Leiden, The Netherlands).

Transport Assays in RSO Membranes. *E. coli* DH5α cells expressing CitS variants were harvested from a 1 L culture by centrifugation at 10000*g* for 10 min at 4 °C. Right-side-out (RSO) membrane vesicles were prepared by the osmotic lysis procedure as described (*25*). RSO membranes were resuspended in 50 mM KP_i, pH 7, rapidly frozen, and stored in liquid nitrogen. Membrane protein concentration was determined by the DC protein assay kit (Bio-Rad Laboratories, Hercules, CA).

Uptake by RSO membranes was measured by the rapid filtration method. The membranes were energized using the K-ascorbate/phenazine methosulfate (PMS) electron donor system (*26*). Membranes were diluted to a final concentration of 0.5 mg/mL into 50 mM KP_i, pH 6.0, containing 70 mM Na^+, in a total volume of 100 μL at 30 °C. Under a constant flow of water-saturated air, and while stirring magnetically, 10 mM K-ascorbate and 100 μM PMS (final concentrations) were added, and the protonmotive force was allowed to develop for 2 min.
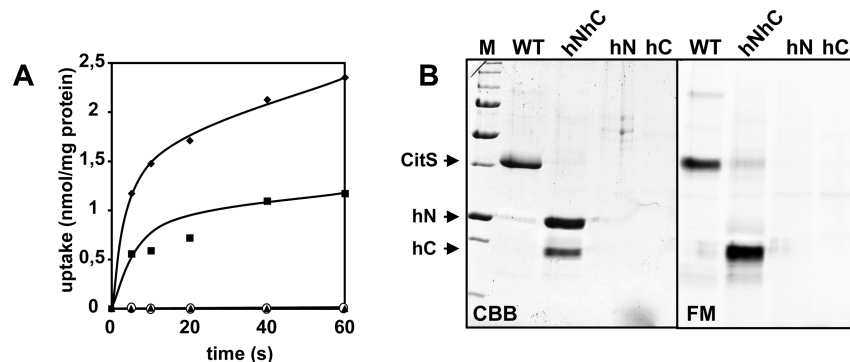
FIGURE 2: Activity and expression of split CitS. (A) [1,5-^{14}C]Citrate uptake by RSO membrane vesicles containing CitS (♦), split CitS-hNhC (■), and the separately expressed domains of CitS, CitS-hN (▲), and CitS-hC (○). (B) SDS−PAGE of purified CitS, split CitS-hNhC, CitS-hN, and CitS-hC after Coomassie Brilliant Blue staining (left panel, CBB) and fluorescence imaging of the same gel (right panel, FM). The gel was loaded with 10 μL of purified CitS eluent and 20 μL for the others. Samples were treated with fluorescein-5-maleimide before running the gel. Arrows point at CitS and the domains hN and hC. Lane M: molecular mass standards. From top to bottom the bands correspond to 200, 150, 100, 75, 50, 37, 25, 20, and 15 kDa. The same marker mix was used in all figures.

Then, [1,5-^{14}C]citrate was added at a final concentration of 4.4 μM. Uptake was stopped by the addition of 2 mL of ice-cold 0.1 M LiCl, followed by immediate filtration over cellulose nitrate filters (0.45 μm, pore size). The filters were washed once with 2 mL of a 0.1 M LiCl solution and assayed for radioactivity. The background was estimated by adding the radiolabeled substrate to the vesicle suspension after the addition of 2 mL of ice-cold LiCl, immediately followed by filtering.

Partial Purification by Ni^{2+}-NTA Affinity Chromatography. E. coli DH5α cells expressing CitS variants were harvested from a 200 mL culture by centrifugation at 10000g for 10 min at 4 °C. Cells were washed with 50 mM KP$_i$ buffer, pH 7, and resuspended in 2 mL of the same buffer and, subsequently, broken by a Soniprep 150 sonicator operated at an amplitude of 8 μm by nine cycles consisting of 15 s on and 45 s off. Cell debris and unbroken cells were removed by centrifugation at 9000 rpm for 5 min. Membranes were collected by ultracentrifugation for 25 min at 80000 rpm at 4 °C in a Beckman TLA 100.4 rotor and washed once with 50 mM KP$_i$, pH 7.0. The membranes (4 mg/mL) were solubilized in 50 mM KP$_i$, pH 8, 400 mM NaCl, 20% glycerol, and 1% Triton X-100 followed by incubation for 30 min at 4 °C under continuous shaking. Undissolved material was removed by ultracentrifugation at 80000 rpm for 25 min at 4 °C. The supernatant was mixed with 40 μL bed volume Ni^{2+}-NTA resin, equilibrated in 50 mM KP$_i$, pH 8.0, 600 mM NaCl, 10% glycerol, 0.1% Triton X-100, and 10 mM imidazole, and incubated overnight at 4 °C under continuous shaking. Subsequently, the column material was pelleted by pulse centrifugation, and the supernatant was removed. The resin was washed with 10 volumes of equilibration buffer containing 300 mM NaCl and 40 mM imidazole. The protein was eluted with 40 μL of the washing buffer containing 150 mM imidazole. The eluted fraction was stored at −20 °C until use. Unless otherwise indicated 20 μL of the eluent was loaded onto a 12% SDS−PAGE gel.

Labeling and Cross-Linking Studies. Aliquots of purified proteins were gently thawed on ice and treated with 0.1 mM fluorescein-5-maleimide (FM) for 5 min at room temperature in the dark. The treatment was stopped with 1 mM DTT. Samples were treated with 2.5 mM glutaraldehyde (GA; Sigma) at room temperature for 20 min. The treatment was quenched with 100 mM Tris-HCl, pH 7.4, after which the samples were left at room temperature for 10 min. In control experiments 0.1% SDS was added to the samples before GA treatment. Samples were

treated with 2 mM sodium tetrathionate (NaTT; Sigma) at 37 °C for 30 min. In control experiments, 5 mM DTT was added to the samples following NaTT treatment. Following treatment, samples were mixed with SDS sample buffer and run on a 12% SDS−PAGE gel. Fluorescent labeling of proteins labeled with FM was visualized on a Fujifilm LAS-4000 luminescent image analyzer (Fuji).

Mass Spectrometry Analysis. Partially purified split CitS variants treated with NaTT were separated by SDS−PAGE using a 12% gel and stained by Coomassie Brilliant Blue. Selected bands were cut from the gel. The pieces of gel were fragmented in smaller pieces, destained in 50 mM ammonium bicarbonate in 40% ethanol, dehydrated by a three times repeated treatment with 100 μL acetonitrile, and dried completely using a SpeedVac centrifuge. The pieces of gel were reswollen by adding 20 μL of a 10 ng/μL trypsin solution, and the samples were incubated overnight at 37 °C. The peptides were extracted from the fluid by shaking for 20 min with 30 μL of a mixture of 60% acetonitrile and 1% trifluoroacetic acid (TFA) in water. The extracted peptides were dried in a SpeedVac centrifuge and dissolved in 10 μL of 0.1% TFA in water. Aliquots of 0.75 μL of the peptide suspension were spotted on the MALDI target and mixed on the target in a 1:1 ratio with the matrix solution consisting of 10 mg/ mL α-cyano-4-hydroxycinnamic acid (dissolved in 70% acetonitrile and 0.1% TFA). The spots were allowed to dry completely before the MALDI-TOF experiment was performed on the Applied Biosystems 4700 proteomics analyzer.

RESULTS

Split CitS Is an Active Transporter. The CitS protein was genetically split in two nonoverlapping polypeptides corresponding to the N- and C-terminal domains (Figure 1). Plasmid pCitS-hNhC contains an artificial operon of two genes, the first one coding for the first 249 amino acids of CitS (TMSI plus the N domain) and the second for the last 198 amino acids (C domain). The operon is under control of the arabinose promoter. The two halves of the *citS* gene were cloned separately, yielding plasmids pCitS-hN and pCitS-hC. In all cases, the encoded polypeptides were extended with six histidine residues (His tag) and an enterokinase side at the N-terminus.

Split CitS-hNhC and the two domains CitS-hN and CitS-hC were tested for the ability to accumulate [1,5-^{14}C]citrate in right-side-out (RSO) membrane vesicles prepared from *E. coli* DH5α
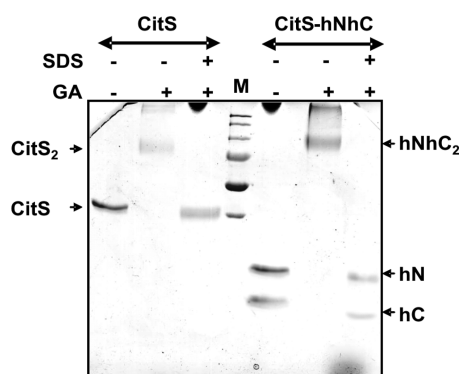
FIGURE 3: Glutaraldehyde cross-linking of CitS and split CitS-hNhC. Purified CitS and split CitS-hNhC were treated with glutaraldehyde (GA) at a concentration of 2.5 mM for 20 min in the presence and absence of 0.1% SDS as indicated at the top followed by SDS−PAGE. Left arrows point at monomeric CitS and dimeric CitS (CitS$_2$). Right arrows point at the domains hN and hC and the tetrameric complex of two N domains and two C domains hNhC$_2$.

cells harboring the appropriate plasmid. Citrate uptake was measured in the presence of a protonmotive force (pmf) that was generated using the artificial electron donor system ascorbate/PMS (Figure 2A). RSO membrane vesicles prepared from cells harboring the empty vector lack citrate uptake activity because of the absence of a citrate transport system in the *E. coli* membrane. RSO membranes prepared from cells coexpressing the two domains retained about 50% uptake activity of membranes containing the wild-type version of CitS. In contrast, membranes prepared from cells expressing the isolated domains did not show any citrate uptake activity.

N-Terminally His-tagged CitS purified by Ni^{2+}-NTA affinity chromatography migrates as a single band with an apparent molecular mass of 38 kDa on SDS−PAGE (Figure 2B, left panel) (*13*, *24*). The coexpressed N and C domains with His tags at the N-termini were purified using the same protocol. On SDS−PAGE two bands showed up with apparent molecular masses of 19 and 25 kDa, strongly suggesting that they correspond to the C domain (198 residues) and N domain (249 residues), respectively. The bands were identified by labeling the purified proteins before SDS−PAGE with fluorescein-5-maleimide (FM), followed by fluorescence imaging of the gel. The CitS protein contains five cysteine residues, all of them located in the C domain. The image showed the labeling of full-length CitS and the 19 kDa band (Figure 2B, right panel). Therefore, the latter corresponds to the C domain. Production of one domain in the absence of the other from constructs pCitS-hN and pCitS-hC was not detected. Apparently, the domains are not stably inserted into the membrane as separate entities.

CitS was shown before to be a dimeric protein by electron microscopy, BN-PAGE, and single molecule fluorescence spectroscopy (*14*, *27*). In agreement, treatment of purified CitS with the unspecific cross-linker glutaraldehyde followed by analysis by SDS−PAGE resulted in complete disappearance of the 38 kDa band and, at the same time, a new, somewhat fuzzy, band appeared running at approximately double the mass (Figure 3). A small fraction of the protein did not enter the gel to any significant extent, suggesting some aggregation in the protein preparation. Treatment with glutaraldehyde in the presence of SDS prevented cross-linking of the protein, showing that cross-linking was the result of complex formation rather than random collisions. The same fuzziness of the band suggests that it is due to
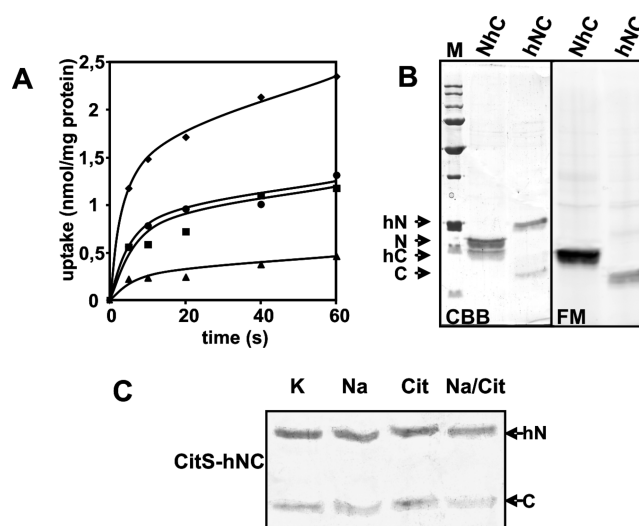

FIGURE 4: Domain interactions in CitS. (A) [1,5-^{14}C]Citrate uptake by RSO membrane vesicles containing CitS (◆), split CitS-hNhC (■), split CitS-hNC (▲), and split CitS-NhC (●). (B) SDS−PAGE of CitS-NhC (NhC) and CitS-hNC (hNC) after Coomassie Brilliant Blue staining (left panel, CBB) and fluorescence imaging of the gel (right panel, FM). Samples were treated with fluorescein-5-maleimide. Arrows indicate the position of the N and C domains with (hN, hC) or without (N, C) a His tag at the N-terminus. (C) SDS−PAGE of CitS-hNC purified in 50 mM KP$_i$, pH 7, in the presence of 200 mM KCl (K), 200 mM NaCl (Na), 10 mM citrate (Cit), and 10 mM citrate plus 200 mM NaCl. Arrows point at the hN and C domains.

random labeling of CitS molecules with glutaraldehyde. Treatment of purified split CitS-hNhC with glutaraldehyde resulted in a similarly sized complex as observed for wild-type CitS indicating a complex consisting of two N and two C domains as in dimeric CitS (Figure 3). Again, treatment with glutaraldehyde in the presence of SDS did not result in cross-linking.

It follows that split CitS, expressed from an artificial operon encoding the two domains as separate proteins, forms a complex of two N domains and two C domains that is active in pmf-driven citrate uptake. The separately expressed domains of CitS are not stably produced, suggesting that the N and C domains stabilize one another.

Domain Interactions in CitS. Two additional vectors encoding the two domains in one operon were constructed to study the interaction between the N and C domains. CitS-hNC represents split CitS with only the N domain His-tagged, while CitS-NhC has only the C domain His-tagged. RSO membrane vesicles prepared from cells expressing the latter showed citrate uptake activity similar to the activity observed for membranes containing split CitS with a His tag at both domains (CitS-hNhC), i.e., about 50% of wild-type CitS activity (Figures 2A and 4A). In contrast, with the His tag only at the N domain (CitS-hNC) the activity was approximately three times lower.

For both combinations, the untagged domain was copurified with the His-tagged domain by Ni^{2+}-NTA affinity chromatography, indicating high affinity between the two domains (Figure 4B, left panel). The N domain of CitS without the His tag migrated on SDS−PAGE at an apparent molecular mass of about 22 kDa while the untagged C domain migrated at 17 kDa. The C domains were identified by FM labeling (Figure 4B, right panel). The expression level of CitS-hNC was clearly lower than observed for CitS-NhC, which is in line with the citrate uptake experiments. Apparently, tagging of the C domain with the His tag and enterokinase site at the N-terminus results in a more stable
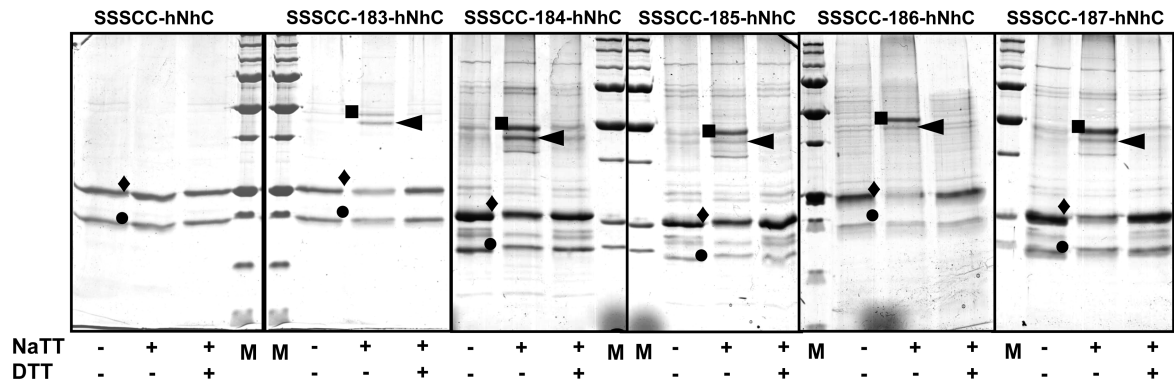
FIGURE 5: Disulfide cross-linking of the reentrant loops in the N and C domains. Split SSSCC-hNhC and split SSSCC variants SSSCC-183-hNhC, SSSCC-184-hNhC, SSSCC-185-hNhC, SSSCC-186-hNhC, and SSSCC-187-hNhC were purified and treated with NaTT, with and without consecutive treatment with DTT as indicated at the bottom followed by SDS−PAGE. (■) Cross-linked N domains, (arrowhead) cross-linked N and C domain, (◆) N domain, and (●) C domain. Mutant protein complexes were isolated from 500 mL cultures, and 30 μL of the eluent was loaded onto the gels.

integration into the membrane. Cross-linking of both variants hNC and NhC by glutaraldehyde resulted in a band of around 80 kDa, indicating that the presence or absence of His tags does not interfere with complex formation (data not shown).

CitS solubilized in detergent has been shown to bind citrate with high affinity (*27*). The interaction between the two domains in the presence of saturating amounts of citrate and the co-ion Na$^+$ was investigated by binding the CitS-hNC and CitS-NhC complexes to Ni^{2+}-NTA resin and washing the columns with buffer containing 10 mM citrate or 200 mM Na$^+$ or both. SDS−PAGE analysis after elution of the His-tagged domain revealed that neither substrate or co-ion did affect copurification of the untagged domain (Figure 4C), suggesting that the binding affinity between the two domains is the same in the free and bound states of the transporter.

Cross-Linking of the Reentrant Loops. The functional complex CitS-hNhC allows for analysis of proximity relationships between the two domains by formation of disulfide cross-links between cysteine residues located in the two domains. Wild-type CitS contains five cysteine residues, all in the C-terminal domain (Figure 2B, right panel). Two of the five cysteines (Cys-398 and Cys-414) are in the putative reentrant loop (Figure 1A, open diamonds) and are important for activity of the transporter, while the other three (Cys-278, Cys-317, and Cys-347) do not seem to play a role in catalysis (*13, 24*). A split version of CitS mutant SSSCC in which the latter three Cys residues were mutated to Ser (*13*) was constructed for cross-linking studies between the N and C domains. RSO membrane vesicles containing SSSCC-hNhC showed 76% of the citrate uptake activity observed with CitS-hNhC, which is similar to that observed before for the SSSCC mutant relative to wild-type CitS (*24*). The drop in activity correlated largely with a lower level of expression (not shown). Treatment of purified SSSCC-hNhC with the oxidant sodium tetrathionate (NaTT) did not result in the appearance of high molecular mass products on SDS−PAGE, showing that no disulfide bonds between two C domains were formed under the conditions of the experiment (Figure 5, left panel).

A set of five single-Cys mutants of the N domain of the split CitS version SSSCC-hNhC was constructed. Each of the amino acid residues in the conserved sequence motif 184-GGNG-187 believed to form the vertex of the reentrant loop (Figure 1A (*8*)), and the glycine residue at position 183 was substituted with a cysteine residue. Then, each mutation results in a SSSCC-hNhC complex with a single cysteine in the putative pore loop in the

Table 1: Citrate Uptake Activities of RSO Membrane Vesicles Containing Reentrant Loop Cys Mutants in Wild-Type CitS and the SSSCC-hNhC Version of CitS

	activity[a] (%)	
mutation	wild-type CitS	SSSCC-hNhC
G183C	95 ± 5	100 ± 4
G184C	12 ± 3^b	9 ± 3
G185C	0 ± 3^b	0 ± 4
N186C	75 ± 5^b	50 ± 7
G187C	12 ± 4^b	9 ± 2

[a]Percentage of the activity observed for wild-type CitS (14.4 nmol/(min·mg of protein)) or the SSSCC-hNhC version of CitS (4.2 nmol/(min·mg of protein)) without the indicated mutations. [b]Data taken from ref *8*.

N domain and two cysteines, Cys-398 and Cys-414, in the reentrant loop in the C domain. The G183C mutation did not affect the uptake activity to a significant extent both in wild-type CitS and in the split SSSCC mutant (Table 1). The mutations in the GGNG motif of the N domain of split SSSCC affected the activity in a similar way as reported before for the same mutations in wild-type CitS (*8*).

Treatment of the five split SSSCC mutants following purification with NaTT under identical conditions as before showed a decrease of the intensity of the two bands corresponding to the N and C domains (Figure 5, ◆ and ●, respectively). The decrease in intensity was stronger for the N domain than for the C domain. Mainly, two new bands showed up running at molecular masses of about 45 and 48 kDa (arrowhead and ■, respectively). Analysis by mass spectrometry identified peptides originating from both the N domain and C domain in the lower 45 kDa band, while the upper 48 kDa band contained peptides of the N domain only. A third minor new band observed with some of the mutants and running at an apparent molecular mass of about 40 kDa was identified as the *E. coli* cAMP receptor protein (CRP) which apparently was present as an impurity in the preparations. It is concluded that the 48 kDa band corresponds to two cross-linked N domains and the 45 kDa band to cross-linked N and C domains of CitS. Cross-linking efficiency between two N domains appears to be more or less the same for all mutants while the efficiency of cross-linking between the N and C domain was higher for the G183 and G184 mutants than observed for the G185, N186, and G187 mutants.

Since CitS is dimeric, the cross-link between the N and C domain in the mutant split SSSCC complexes may be formed

between the domains of one subunit or between the domains of different subunits. Obviously, the cross-link between the N domains is between different subunits. Mutants of "full-length" CitS were constructed containing the G183C and N186C mutants in the SSSCC background. No cross-linking was detected between the subunits upon treatment of the purified proteins with NaTT, demonstrating that the cross-link between the N and C domain is in one subunit and the cross-link between the two N domains is only observed in the split CitS constructs (data not shown). The results support a close proximity of reentrant loops Vb and Xa (Figure 1A) in the N and C domain of one subunit of dimeric CitS.

DISCUSSION

The structural model of the CitS transporter of *K. pneumoniae* shows two homologous domains, each containing five TMSs, with inverted topology in the membrane (*2*, *15*). Prominent in the model are two reentrant loops connecting the fourth and fifth TMSs in each domain that fold back in between the TMSs from opposite sides of the membrane (*trans*-reentrant loops). The reentrant loop regions are highly conserved in the 2HCT family and contain a sequence motif GGXG that was shown to be essential for activity of the transporter (*8*). By analogy to other two-domain transporter structures (*19*, *20*, *28−30*), it was proposed that the translocation site would be formed at the interface of the two domains and, consequently, the two reentrant loops would be positioned at the interface. In this study we present evidence that the reentrant loops are in close vicinity in the 3D structure. In the purified transporter complex, cysteine residues engineered in the reentrant loop in the N domain (VB, Figure 1A) were shown to form a disulfide bond with either of two endogenous cysteine residues in the reentrant loop in the C domain (XA, Figure 1A, open diamonds). The disulfide bond cross-linked the N and C domains in a split version of CitS, but not the subunits in "full-length" CitS, indicating that in dimeric CitS (*14*) the reentrant loops of the same subunit are in close contact. In the N domain, the cysteine residues involved in the cross-links were positioned at the 184-GGNG-187 sequence motif that is believed to be at the vertex of the reentrant loop (*8*). They cross-link to cysteine residues Cys398 and/or Cys414 positioned at the base of the reentrant loop in the C domain where the sequence motif is 403-GGSG-406. Apparently, the two loops overlap one another at the domain interface, suggesting that they may constitute a major part of the wall of the translocation pore (Figure 6). Accessibility of a Cys residue substituting for Ser405 in sequence motif 403-GGSG-406 by the bulky, membrane-impermeable thiol reagent 4-acetamido-4′-maleimidylstilbene-2,2′-disulfonic acid (AMdiS) from the periplasmic side of the membrane demonstrated previously (*8*) is the best evidence for the reentrant loop in the C domain to stick through the membrane all the way. The accessibility of Cys residues at positions 398 and 414 from the periplasm was shown to be restricted to small thiol reagents such as [2-(trimethylammonium)ethyl]methanethiosulfonate bromide (MTSET (*24*),) suggesting that they are located deeper in a narrower part of the pore from a periplasmic perspective. The disulfide cross-links to the latter demonstrated here represent the first experimental evidence that the putative reentrant loop in the N domain may actually enter the membrane-embedded part of the protein as depicted in Figure 6. At consecutive positions 183 through 187, the highest cross-linking efficiency was observed with Cys residues at positions 183 and 184, suggesting that
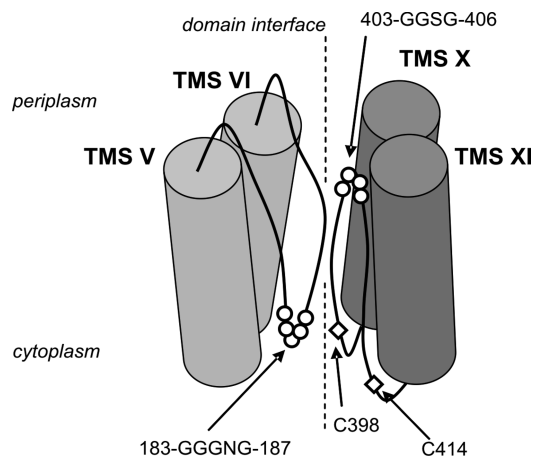

FIGURE 6: Structural model of the domain interface of CitS of *K. pneumoniae*. Shown are TMSs V and VI in the N domain and TMSs X and XI in the C domain together with the connecting reentrant loops. See text for further explanation.

movement of the tip of the loop is constrained by the conformation of the protein.

The disulfide bond formed between the putative reentrant loops of CitS upon oxidation was identified by cross-linking the two domains in a split version of CitS in the detergent-solubilized state which may not necessarily reflect the structure of wild-type CitS embedded in the membrane. Cross-linking artifacts might occur because of increased flexibility of the polypeptide chain and instability of the complex in detergent solution and because of misfolding of (part of) the split transporter. Several observations argue against such artifacts in this particular case. (i) Individually expressed N and C domains could not be detected in the membrane (Figure 2). The same result was obtained before for a split version of the lactose transporter LacY of *E. coli* (*23*, *31*). (ii) Only a single complex containing two N domains and two C domains corresponding to dimeric CitS was detected in the solubilized state (Figure 3). Titration of purified split CitS with increasing concentrations of the nonspecific cross-linker glutaraldehyde resulted in two intermediate bands on SDS−PAGE in the lower concentration domain (data not shown). The bands disappeared at higher concentrations of glutaraldehyde to yield the single cross-linked product shown in Figure 3. (iii) The interaction between the domains in the solubilized state is very strong. Binding of one domain to Ni^{2+}-NTA affinity resin through an engineered His tag resulted in copurification of the other domain (Figure 4). The copurified domain could not be eluted by extensive washing under different conditions unless nonphysiological conditions were used (not shown). The high affinity between the domains was not affected by the presence of saturating amounts of substrate and co-ions of the transporter (Figure 4C). It follows for the split CitS variant that only the complex corresponding to the original CitS dimer is stably integrated in the membrane and purified in detergent solution. Apparently, any N or C domain produced in excess is being digested by the proteolytic system of the cells, and in all likelihood, the single complex observed in detergent solution is the same structure as present in the membrane that is responsible for transport activity. Increased flexibility of the complex in detergent solution could result in proximities of sites that would be more distant in the membrane. But, it is highly unlikely that within this complex, because of increased flexibility, a periplasmic loop would cross-link to a cytoplasmic loop (*trans* reentrant loops).

The split CitS complex consists of two N and two C domains in an arrangement as in dimeric CitS. In addition to cross-linking of the N and C domains within one subunit, the same split CitS variants resulted in cross-linking of two N domains. The cross-link must be the result of disulfide formation between the single cysteine residues in the reentrant loops in the N domains and correspond to an intersubunit cross-link. Nevertheless, cross-linking of purified CitS to a dimer was not observed when the single Cys183 and Cys186 variants of "full-length" CitS were treated with NaTT under the same conditions, suggesting that cross-linking of two N-domains is an artifact of the split versions of CitS. The conclusion is supported by the lack of specificity of cross-linking efficiency for the cysteine residues at the different positions in the reentrant loop. One possible scenario might be that a fraction of the reentrant loops in the N domain are not properly inserted in the membrane-embedded part of the complex as a consequence of the different biogenesis route for split CitS. Assembly follows after insertion of the two protein halves at different sites in the membrane. Possibly, proper insertion of the reentrant loop in the N domain requires the coordinated insertion of the C domain which is the normal situation when CitS is synthesized from a single gene. The assisted insertion of TMS VIII of CitS by downstream TMS IX that was reported before (*32*) provides a precedent for a mechanism by which proper insertion of the reentrant loop in the N domain would depend on C-terminal sequences in CitS.

ACKNOWLEDGMENT

REFERENCES

1. Saier, M. H., Jr. (2000) A functional-phylogenetic classification system for transmembrane solute transporters. *Microbiol. Mol. Rev. 64*, 354–411.
2. Sobczak, I., and Lolkema, J. S. (2005) The 2-hydroxycarboxylate transporter family: physiology, structure, and mechanism. *Microbiol. Mol. Biol. Rev. 69*, 665–695.
3. Lolkema, J. S., and Slotboom, D. J. (1998) Estimation of structural similarity of membrane proteins by hydropathy profile alignment. *Mol. Membr. Biol. 15*, 33–42.
4. Lolkema, J. S., and Slotboom, D. J. (1998) Hydropathy profile alignment. A tool to search for structural homologues of membrane proteins. *FEMS Microbiol. Rev. 22*, 305–322.
5. Lolkema, J. S., and Slotboom, D. J. (2003) Classification of 29 families of secondary transport proteins. *J. Mol. Biol. 327*, 901–909.
6. Lolkema, J. S., and Slotboom, D. J. (2005) Sequence and hydropathy profile analysis of two classes of secondary transporters. *Mol. Membr. Biol. 22*, 177–189.
7. Lolkema, J. S., and Slotboom, D. J. (2008) The major amino acid transporter superfamily has a similar core structure as Na⁺-galactose and Na⁺-leucine transporters. *Mol. Membr. Biol. 25*, 567–570.
8. Dobrowolski, A., and Lolkema, J. S. (2009) Functional importance of GGXG sequence motifs in putative reentrant loops of 2HCT and ESS transport proteins. *Biochemistry 48*, 7448–7456.
9. Dobrowolski, A., Sobczak-Elbourne, I., and Lolkema, J. S. (2007) Membrane topology prediction by hydropathy profile alignment: membrane topology of the Na⁺-glutamate transporter GltS. *Biochemistry 46*, 2326–2332.
10. ter Horst, R., and Lolkema, J. S. (2009) Rapid screening of membrane topology of secondary transport proteins. *Biochim. Biophys. Acta 1798*, 672–680.
11. Prakash, S., Cooper, G., Singhi, S., and Saier, M. H., Jr. (2003) The ion transporter superfamily. *Biochim. Biophys. Acta 1618*, 79–92.
12. van Geest, M., and Lolkema, J. S. (2000) Membrane topology of Na(+)/citrate transporter CitS of *Klebsiella pneumoniae* by insertion mutagenesis. *Biochim. Biophys. Acta 1466*, 328–338.
13. Sobczak, I., and Lolkema, J. S. (2004) Alternating access and a pore-loop structure in the Na⁺-citrate transporter CitS of *Klebsiella pneumoniae*. *J. Biol. Chem. 279*, 31113–31120.
14. Mościcka, K. B., Krupnik, T., Boekema, E. J., and Lolkema, J. S. (2009) Projection structure by single-particle electron microscopy of secondary transport proteins GltT, CitS, and GltS. *Biochemistry 48*, 6618–6623.
15. Lolkema, J. S., Sobczak, I., and Slotboom, D. J. (2005) Secondary transporters of the 2HCT family contain two homologous domains with inverted membrane topology and trans re-entrant loops. *FEBS J. 272*, 2334–2344.
16. Lolkema, J. S. (2006) Domain structure and pore-loops in the 2-hydroxycarboxylate transporter family. *J. Mol. Microbiol. Biotechnol. 11*, 318–325.
17. Fu, D., Libson, A., Miercke, L. J., Weitzman, C., Nollert, P., Krucinski, J., and Stroud, R. M. (2000) Structural determinants of water permeation through aquaporin-1. *Science 290*, 481–486.
18. Hunte, C., Screpanti, E., Venturi, M., Rimon, A., Padan, E., and Michel, H. (2005) Structure of the Na⁺/H⁺ antiporter and insight into mechanism of action and regulation by pH. *Nature 435*, 1197–1202.
19. Khademi, S., O'Connell, J., III., Remis, J., Robles-Colmenares, Y., Miercke, L. J. W., and Stroud, R. (2004) Mechanism of ammonia transport by Amt/MEP/Rh: structure of AmtB at 1.35 Å. *Science 305*, 1587–1594.
20. Yamashita, A., Singh, S. K., Kawate, T., Jin, Y., and Gouaux, E. (2005) Crystal structure of a bacterial homologue of Na⁺/Cl⁻-dependent neurotransmitter transporters. *Nature 437*, 215–223.
21. Lolkema, J. S., Dobrowolski, A., and Slotboom, D. J. (2008) Evolution of antiparallel two-domain membrane proteins: tracing multiple gene duplication events in the DUF606 family. *J. Mol. Biol. 378*, 596–606.
22. Yernool, D., Boudker, O., Jin, Y., and Gouaux, E. (2004) Structure of a glutamate transporter homologue from *Pyrococcus horikoshii*. *Nature 431*, 811–818.
23. Bibi, E., and Kaback, H. R. (1990) *In vivo* expression of the *lac Y* gene in two segments leads to functional *lac* permease. *Proc. Natl. Acad. Sci. U.S.A. 87*, 4325–4329.
24. Sobczak, I., and Lolkema, J. S. (2003) Accessibility of cysteine residues in a cytoplasmic loop of CitS of *Klebsiella pneumoniae* is controlled by the catalytic state of the transporter. *Biochemistry 42*, 9789–9796.
25. Kaback, H. R. (1974) Transport in isolated bacterial membrane vesicles. *Methods Enzymol. 31*, 698–709.
26. Konings, W. N., Barnes, E. N., Jr., and Kaback, H. R. (1971) Mechanisms of active transport in isolated membrane vesicles. 2. The coupling of reduced phenazine methosulfate to the concentrative uptake of β-galactosides and amino acids. *J. Biol. Chem. 246*, 5857–5861.
27. Kastner, C. N., Prummer, M., Sick, B., Renn, A., Wild, U. P., and Dimroth, P. (2003) The citrate carrier CitS probed by single-molecule fluorescence spectroscopy. *Biophys. J. 84*, 1651–1659.
28. Shaffer, P. L., Goehring, A., Shankaranarayanan, A., and Gouaux, E. (2009) Structure and mechanism of a Na⁺-independent amino acid transporter. *Science 325*, 1010–1014.
29. Abramson, J., Smirnova, I., Kasho, V., Verner, G., Kaback, H. R., and Iwata, S. (2003) Structure and mechanism of the lactose permease of *Escherichia coli*. *Science 301*, 610–615.
30. Huang, Y., Lemieux, M. J., Song, J., Auer, M., and Wang, D. N. (2003) Structure and mechanism of the glycerol-3-phosphate transporter from *Escherichia coli*. *Science 301*, 616–620.
31. Wu, J., and Kaback, H. R. (1996) A general method for determining helix packing in membrane proteins *in situ*: helices I and II are close to helix VII in the lactosepermease of *Escherichia coli*. *Proc. Natl. Acad. Sci. U.S.A. 93*, 14498–14502.
32. van Geest, M., and Lolkema, J. S. (1999) Transmembrane segment (TMS) VIII of the Na(+)/citrate transporter CitS requires downstream TMS IX for insertion in the *Escherichia coli* membrane. *J. Biol. Chem. 274*, 29705–29711.